FRACTURE ENERGY ANALYSIS VIA ACOUSTIC EMISSION

L.I. Maslov and V.V. Sukharevsky*

The results of previous studies on acoustic emission during loading are used to relate the characteristics of the acoustic signals to the fracture processes occurring at the crack tip. It is shown that all emissions correspond to the formation of individual microfractures, to the process of macroplastic deformation and to stepwise crack propagation of the structurally disordered material, respectively.

Load of solids leads to formation of cracks and fracture of its inner structure. This process connected with break of adhesive and cohesive bonds,is a reason for violation of the electric neutrality of the crack walls and leads to different emissions. The emissions start during crack propagation and in some cases after fracture of material. It includes the emission of charged particles (1-7), neutral molecules or their unity (8), electromagnetic wave difference frequency (9-12), which follows interaction of electrons with atoms of solids. All these emissions of a crack due to mechanic pressure and all these phenomena have a common mechanism called "fracto-emission" (FE) (4). Crack propagation is followed by elastic stress waves causing acoustic emission (AE). It gives information about the process in the local volume near the crack tip (13). A maximum intensity of FE and AE is observed within one crack jump. For different solids these emission times vary from microseconds to less.

* A.A. Baikov Institute of Metallurgy,
U.S.S.R. Academy of Sciences, Moscow, V-334, Leninsky pr. 49.

In the zone of crack propagation the effect of charge separation is observed. These effects produce great electric fields that can achieve 10 - 30 kV $\cdot$ cm^{-1} (10). These fields lead to electron emission from the crack wall and accelerate electrons from 5 - 10 ev to 10 kev. Under different conditions parts having as high as 100 kev have been observed coming from alkali halides (5).

Let us estimate the maximum energy at the moment of the crack jump. Atom ionisation is available mainly on the surface of the walls and is accounted for fracture energy. There are $N \sim 10^{15}/cm^2$ atoms in a layer of solid with thickness of 1 Å. The number of valence electrons for different elements varies from 1 to 5. Let us consider a case when atom loose only one external electron. In this case a charge is formed on the surface with a square of 1 cm^2:

$$Q_{sur} = e \cdot N = 1.6 \times 10^{-4} \quad C \cdot cm^{-2} \qquad (1)$$

where e is charge of electrons.

This result shows that this is a limit case because the charge produces electrical fields of $E = 10^6 - 10^7$ V $\cdot$ cm^{-1} and autoelectronics emission begins.

Production of highly localized heat (13) as a result of atomic bond fracture provides thermo-electronic emission under low electrical fields. This heat results in excitement of atoms and electrons in form of infra-red spectrum photons.

The process of energy emission (figure 1) can result in: electromagnetic waves, electrical fields, FE, AE and other low energy processes depending on type and energy between atomic bonds. This atomic bonds can be covalence, ionic, metallic or hydrogen type, Van der Waals bond. The strongest atomic bonds are: covalence, ionic, metallic which are broken when the material is destroyed and much energy is generated.

Acoustic emission signals are classified according to their duration into continuous and discrete types. Continuous emission is characterized by low amplitude and high frequency, while for discrete emission the signals are of high amplitude and low frequency. A minimum pulse duration for the AE to be referred to as continuous has been agreed (14), (15).

From the data obtained in the authors experiments on specimens and pressure vessels (16), it has been shown that, depending on the loading conditions, the amplitude distribution of AE signals may be approximated by either the Rayleigh or Gaussian law

for random values, while a power function describes the decrease in the number of pulses with increasing amplitude. Therefore it has been inferred that a monotonically decreasing function $N_i = f(n_i)$ must describe the discrete AE whereas continuous or quasi-stationary AE signals must be characterized by a function with a maximum $N_i = f(n_i)$.

Discrete AE signals are observed at $\sigma_i < \sigma_{ys}$. These signals can be described or approximated by differential and integral power functions:

$$N_i = A\, n^{-b} \tag{2}$$

$$\Sigma N = B\, n^{-a} \tag{3}$$

where N_i is the number of pulses with amplitude n_i or ΣN_i is the total number of pulses with an amplitude greater than n_i, respectively.

Eccentric tension tests on notched and fatigue cracked specimens have shown (16), (17) that not only does the AE count change with loading, but more importantly the character of the AE signals changes accordingly. For Cr-Mo steel grades of average strength, it has been established that:

- below the yield point ($\sigma_i < \sigma_{ys}$) $N_i = f(n_i)$ is a monotonically decreasing function described by equations (2) and (3) where a = 0,7-3,5 and b = 1,47-1,5. AE signals are discrete or random
- where the stress is near to that of the yield point ($\sigma_i \approx \sigma_{ys}$), the function $N_i = f(n_i)$ exhibits a peak. The signals are those of continuous acoustic emission
- at stresses considerably greater than that at the yield point ($\sigma_i > \sigma_{ys} \approx \sigma_F$), the amplitude distribution function resumes the discrete character it has below the yield point (figure 2).

The fact that the distribution of AE counts below and above the yield point can be described by power functions indicates the occurrence in both cases of random events with zero mean value and standard deviation equal to one. Evidently, the amplitude or power of AE signals is quite different at $\sigma_i < \sigma_{ys}$ and $\sigma_i > \sigma_{ys}$. However, the narrow amplitude distribution of counts in both cases implies that they are produced by AE nucleation sites of nearly the same energy release density.

In the continuous AE that fits the Gaussian model at $\sigma_i \approx \sigma_{ys}$, there is a great amount of superposition of random events, i.e. AE signals differing in power and amplitude. This phenomenon is accounted for by the high density of AE counts near the yield point, conventionally perceived as continuous. Thus, in the strained crack tip region bounded by the condition $\sigma_i \approx \sigma_{ys}$, one should expect signals of both high and low amplitude not only because they have different sources, but because they are asynchronous.

From the data obtained it may be concluded that when $\sigma_i < \sigma_{ys}$, individual fracture sites exist that generate low amplitude AE signals of roughly the same power. With increasing stress these fracture sites grow in number and density until a maximum is reached near the density corresponding to the yield point, when macroplastic deformation occurs at the crack tip. During the stage of discrete crack propagation or crack jumping when $\sigma_i > \sigma_{ys}$, AE signals are generated either in small series or as individual pulses with high amplitude. This type of emission is due to the discrete character of the fracture of small volumes of metal at the tip which are in a state of structural disorder.

Therefore, the type of AE signal must be related to the level of stress as well as to the volume of crack tip material involved in the micro- and macroplastic deformation of fracture. In other words, the diversity of acoustic emission indicated that crack tip plastic deformation is a discontinuous, stage-by-stage process leading to discrete failure.

Let us now consider the AE activity in a fatigue precracked compact specimen under tension loading. AE analysis combined with fractographic investigations have shown that at $\sigma_i < \sigma_{ys}$ a "go-off" zone of individual microfracture sites can be identified as the crack tip macroplastic strain region.

Depending on the stress level, the homogeneity of structural components and the internal energy, fracture sites occur in areas of unfavourably located or oriented grains, subgrains or particles of the second phase at stress concentrators. Thus AE sources are randomly distributed in the crack tip area, while the generation of AE signals is of a quasi-stationary character described by the σ_{AE} value.

The authors results show that the local microfracture zone size L_{AE} as determined via AE analysis, is proportional to the applied stress, or:

$$\sigma_{AE}^2 L_{AE} = \text{constant} \qquad (4)$$

where σ_{AE}, the stress corresponding to the start of AE, is constant for an alloy with a given base. During loading, the area of AE generation constantly changes in size, while the integral of σ^2_{AE} over the line L(t) (limiting this area) remains constant.

Numerous fractographic investigations have related a macrostriation pattern on the fracture surface of compact specimens loaded to failure under various loading conditions, provided that the material exhibits elastic-plastic behaviour (figure 3).

Each striation is formed when the crack front stops during discrete or stepwise crack propagation, the distants jumped being equal to the size of the irreversible deformation zone, $2r_{ys}$ (13).

Microstructural analysis has confirmed the existence of a maximum strain or failure zone ($2r_F$) between macrostriation ridges. Data obtained via this type of analysis indicate that the formation of the irreversible plastic deformation zone ($2r_{ys}$) is accompanied by continuous acoustic emission fitting the Gaussian model. In addition statistical analysis of experimental data on dimple relief in the $2r_F$ zone shows that this particular kind of fracture is characterized by dimples with inclusions on their bottoms. From this observation it follows that the particles are located in hollows.

The density of the specific energy released during cracking near inclusion and the formation of a fracture "quantum" may be expressed as:

$$S_c = \frac{\gamma_c}{d} \qquad (5)$$

where S_c is the density of released specific energy, γ_c is the specific energy released during formation of the fracture quantum and d is the critical size of the quantum. Calculations shows that the value of S is close to or more than that of the absolute latent heat of melting, which is released on the transition of the metal into a premelted or pseudomelted state (13). This implies that in this zone the material must be in structural disorder or in the premelted state, causing the release of a powerful pulse of excess internal energy in the form of heat and AE.

This discrete high amplitude acoustic emission signals are provided during crack jumping when the material at the crack tip is in a state of structural disorder.

Analysis of AE phenomena of a thermofluctuation character has shown that the generation of heat in a narrow area of the crack

tip significantly affects the AE pattern, causing a proportional increase in the AE intensity from the 2r zone and to its decrease as heat dissipation. This change in the character of AE intensity with time suggests that the duration of the fracture quantum is determined by the rate of heat transfer in the material, i.e. by heat conduction, melting heat and heat capacity.

The observation of a powerful AE pulse per unit time testifies the formation of a fracture quantum possessing the following specific features:

- the energy released per unit time is proportional to the melting temperature
- the fill-in frequency of the pulse is characteristic of the photon area of the solid body spectrum
- due to heat condition, the envelope of the pulse describes the temperature fall at the crack tip and is a monotonically decreasing function of time (figure 4).

CONCLUSIONS

Acoustic emission data obtained during testing are analysed and shown to reveal the inhomogeneity of the plastic strain region at the crack tip. From the observed analysis of experimental data it follows that there is a common reason for all emission phenomena that is for FE and AE, which is connected with atomic bond energy concentration and generation. This energy is generated in a local zone near the crack tip under deformation and fracture.

FE intensity depends only on interatomic interaction energy and on the rate of its generation. During a short period of time equal to the duration of a crack jump we observe the following: local electromagnetic field generation in the form of infra-red photons, electrical field, FE, acoustic emission and so on.

These processes start simultaneously which is proved by the simultaneous electron and acoustic emission (7) at the moment of crack jump. Starts before crack jumped AE and is maximum in the moment of fracture, than it falls down abruptly. The coincidence of AE maximum and the starting of electron emission (figure 5) show that first there is an accumulation of defects in the solid to be followed by fracture and FE.

Since the decrease of free crack walls is followed by FE, it is very sensitive to subcritical propagation and allows to define early stages of deformation kinds and fracture in solids. Investigation of electron, ion emission and x-ray emission allow to determine fracture mechanism and fracture properties of materials. We shall also be able to interprete acoustic emission data and to locate micro defects before fracture.

For application of various emission types as a method of early fracture diagnostics, we suppose that FE with AE is the only experimental method to investigate the dynamics of formation and jump propagation of microcracks.

REFERENCES

(1) Karasev, V.V., Krotova, N.A. and Deriaguin, B.D., Reports AN U.S.S.R., Fisika, 1953, t.LXXXVIII, No. 5, pp. 777-780 (in Russian).

(2) Deriaguin, B.D., Krotova, N.A.and Smilga, V.P., Adgezia Tverdih Tel, M., Nauka, 1973, pp. 280 (in Russian).

(3) Rosenlum, B.Z., Bräunlich, P.F. and Himmel, L., J. Apple. Phys.,No. 48, 1977, pp. 5262.

(4) Dickinson, J.T., Donaldson, E.E.and Park, M.K., J. Mater. Sci., No. 16, 1981, pp. 2897-2908.

(5) Wollbrandt, J., Linke, E. and Meyer, K., Phys. Stat. Sol. (A), K 53, 1975.

(6) Dickinson, J.T., Bräunlich, P.F., Larson, L., Marceau, A., Appl. Surf. Sci., No. 1, 1978, pp. 515.

(7) Dickinson, J.T., Janan-Latibari, A. and Jensen, L.C., J. Mater. Sci., NO. 20, 1985, pp. 229-236.

(8) Larson, L.A., Dickinson, J.T., Bräunlich, P.F. and Snyder, D.B., J. Vac. Sci. Technol., No. 18, 1980, pp. 238.

(9) Gorazdovsky, T.J., Prisma Jatf., TS, No. 78, 1967, pp. 78-82.

(10) Anisimova, V.I., Kluev, V.A., Vladikina, T.N., Krotova, N.A., Toporov, J.P. and Deriaguin, B.V., Reports AN U.S.S.R. Fisicheskaya Himia, YT, No. 233, 1977, pp. 140-143 (in Russian).

(11) Kluev, V.A., Lipson, A.G., Toporov, O.P., Aliev, A.D., Chalykh, A.E. and Deriaguin, B.V., Report AN U.S.S.R. Fisicheskaya Himia, T. 279, No. 2, 1984, pp. 415-419 (in Russian).

(12) Rosenblum, B., Bräunlich, P.F. and Cappico, J.P., Appl. Phis. Lett., Vol. 25, No. 1, 1974, pp. 17-19.

(13) Maslov, L.I. and Gradov, O.M., Int. J. Fatigue, Vol. 7, No. 2, 1986.

(14) Radon, J.C. and Pollock, A.A., Engng. Fract. Mech., Vol. 4, 1972, pp. 295-310.

(15) Rogers, L.M. and Monk, R.G., 2nd Nat. Conf. on Cond. Monit. Process Int., London, U.K., 10-11 May, 1983, pp. 1-24.

(16) Maslov, L.I., Paper of Ship Research Institute, No. 60, Tokyo, Japan, 1980.

(17) Maslov, L.I., Voprosi Atomnoi Nauki i Tekhniki, M., NIKIMT, 1, 1983, pp. 4-10(in Russian).

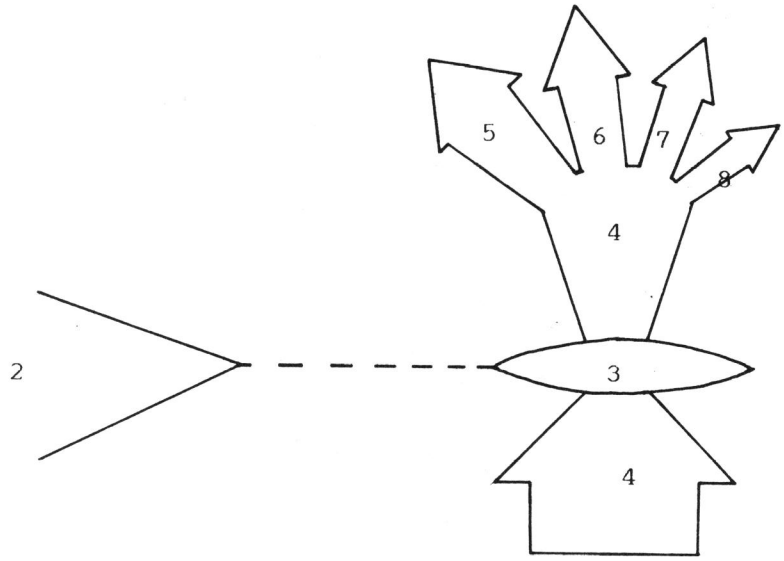

Figure 1 Diagram of loading and energy generation under fracture of solids.

1. Mechanic energy
2. Crack
3. Point of precritical crack propagation or fracture zone
4. Energy between atomic bond
5. Electromagnetic waves
6. Electric fields
7. FE
8. AE

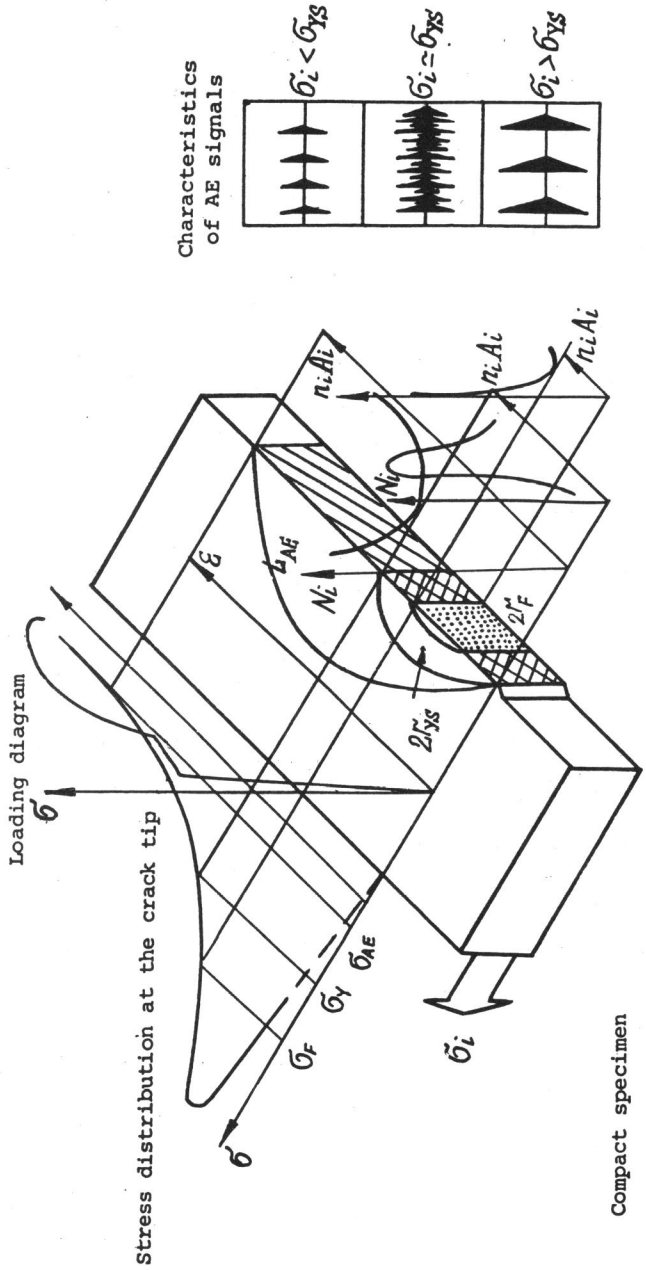

Figure 2 The variation of AE signals (amplitude distribution) with loading (stress) condition

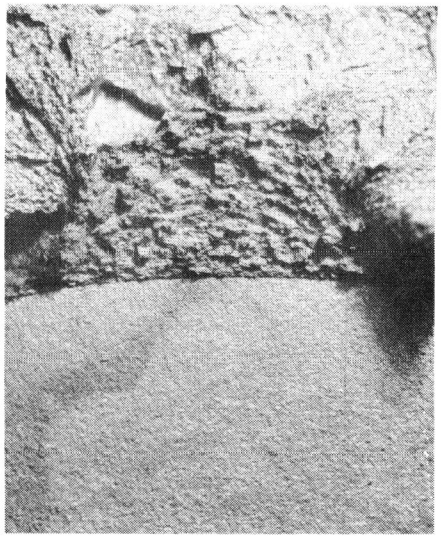

Figure 3 The fracture surface of a compact specimen
A = peak amplitude
D = signal duration
N = number of counts per event
R = rise time
U = energy (proportional to the square of amplitude)
$U_{max} \sim T_m$ proportional to melting temperature
$U(t) \sim T(t)$ proportional to temperature
$\omega_s = 2\pi N/D$ frequency

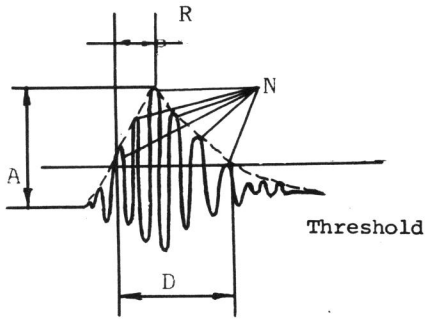

Figure 4 Schematic of a powerful AE signal

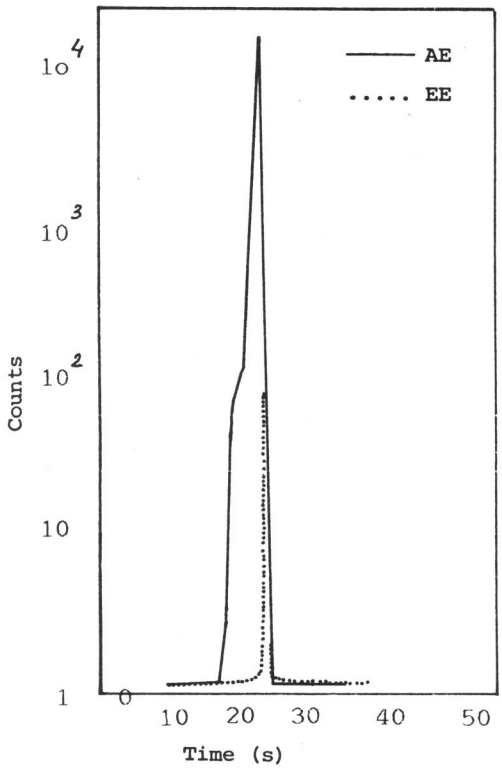

Figure 5 The EE and AE accompanying the flexural straining of a (90) graphite-epoxy composite (7).